INTERNATIONAL ATOMIC ENERGY AGENCY
UNITED NATIONS EDUCATIONAL, SCIENTIFIC AND CULTURAL ORGANIZATION

INTERNATIONAL CENTRE FOR THEORETICAL PHYSICS
34100 TRIESTE (ITALY) - P.O.B. 586 - MIRAMARE - STRADA COSTIERA 11 - TELEPHONE: 2240-1
CABLE: CENTRATOM - TELEX 460392-1

SMR/169 -14

WORKSHOP ON OPTICAL FIBER COMMUNICATION
(24 February - 21 March 1986)

# NONLINEAR PHENOMENA IN OPTICAL FIBERS

presented by

B. CROSIGNANI
Fondazione "Ugo Bordoni"
Viale Europa, 190
00144 Roma
Italy

# NONLINEAR PHENOMENA IN OPTICAL FIBERS

B.CROSIGNANI

*Dipartimento di Fisica Universita' di Roma and Fondazione "Ugo Bordoni" - Roma Italy.*

## Introduction

*The advent of extremely low-loss single-mode optical fibers and the availability of laser transmitters of increased power points towards a situation in which nonlinear optical effects are becoming more and more important in determining the propagation characteristics of the fiber itself. In fact, also if the nonlinear optical properties of silica are rather poor, the long interaction length provided by the fiber more than compensate for this circumstance, as it can be easily understood by comparing the "strength" of the nonlinear interaction in a bulk medium and in a waveguide structure (see Fig.1). In fact, we have in the two cases that the intensity one can achieve is given by* $I_b = P/\pi b^2$ *and* $I_f = P/\pi a^2$ *where* $b$ *and* $a$ *are respectively the radius of the beam spot-size and of the fiber; however, while in the last situation the beam remains confined for a length L equal to the fiber length , in the first case, due to diffraction, the interaction with the nonlinear medium is basically limited to a region of length* $L_i = \pi b^2/\lambda$. *The ratio between the strength of the two interactions, which can be assumed to be proportional to the product of the light intensity and the interaction length, is than given by*

$$\frac{I_f L}{I_b L_i} = \frac{\lambda L}{\pi a^2} \sim \frac{L}{a}$$



*and it is clearly favourable to guided propagation since L/a can be easily made very large (*$10^5 \div 10^6$ *for a fiber few meters long). The above argument leads one to expect that, over fiber lengths of several kilometers, nonlinear effects can really become the most influent in determining the performances of a telecommunication link. Actually, the onset of optical nonlinearities produces a variety of effects which, if on one hand constitute a limiting factor for the transmission potentialities of the fiber, on the other hand can be exploited for achieving special propagation characteristics (e.g. pulse compression and solitons) which in turn could be expedient for realizing very wide band transmission systems. Besides, a completely new field is now being developed which takes advantage of the fiber nonlinearities for obtaining new kinds of optical devices (e.g., fiber Raman lasers) operating at low power levels.*

## Nonlinear optical susceptibilities

*The response of a dielectric medium to an applied field* $\underline{E}(t)$ *can be expressed, in the time domain, through the following relation between the polarization vector* $\underline{P}(t)$ *and the field itself:*

$$\underline{P}_i(t) = \underline{P}_i^{(1)}(t) + \underline{P}_i^{(2)}(t) + \underline{P}_i^{(3)}(t) + \cdots\cdots =$$

$$\sum_{j=1}^{3} \int_{-\infty}^{+\infty} \chi_{ij}^{(1)}(t-\tau) E_j(\tau)\, d\tau + \sum_j \sum_k \iint_{-\infty}^{+\infty} \chi_{ijk}^{(2)}(t-\tau_1, t-\tau_2) E_j(\tau_1) E_k(\tau_2)\, d\tau_1 d\tau_2 \quad (1)$$

$$+ \sum_j \sum_k \sum_\ell \iiint_{-\infty}^{+\infty} \chi_{ijk\ell}^{(3)}(t-\tau_1, t-\tau_2, t-\tau_3) E_j(\tau_1) E_k(\tau_2) E_\ell(\tau_3)\, d\tau_1 d\tau_2 d\tau_3 + \cdots\cdots \,, \quad i=1,2,3.$$

*In Eq.(1), which includes terms of decreasing importance in the electric field strength, the dielectric medium is characterized by the response tensor* $\chi_{ijk\ldots}^{(m)}$ . *In particular, for m=1, one obtains the linear theory of dielectrics*

described by the relation

$$P_i^{(1)}(t) = \sum_{j=1}^{3} \int_{-\infty}^{+\infty} \chi_{ij}^{(1)}(t-\tau) E_j(\tau) d\tau \quad , \quad i = 1,1,3 \quad , \qquad (2)$$

or, in the frequency domain (we indicate with $\tilde{f}(\omega)$ the Fourier transform of $f(t)$),

$$\tilde{P}_i^{(1)}(\omega) = \sum_j \tilde{\chi}_{ij}^{(1)}(\omega) \tilde{E}_j(\omega) \quad , \quad i = 1,2,3 \quad , \qquad (3)$$

which allows in particular to define the dielectric – constant tensor $\varepsilon_{ij}(\omega)$ through the equation

$$\tilde{D}_i(\omega) = \varepsilon_0 \tilde{E}_i(\omega) + \tilde{P}_i^{(1)}(\omega) = \sum_j \varepsilon_0 \left[ \delta_{ij} + \tilde{\chi}_{ij}(\omega) \right] \tilde{E}_j(\omega)$$
$$= \sum_j \varepsilon_{ij}(\omega) \tilde{E}_j(\omega) \quad , \quad i = 1,2,3 \quad , \qquad (4)$$

where $\varepsilon_0$ is the vacuum permittivity.

In the frame of optical fibers, the main concern is with isotropic media (e.g., silica), which possess macroscopic inversion symmetry, that is whose structure remains unchanged by replacing the coordinate $\underline{r}$ by $-\underline{r}$. In this case, the nonlinear response tensor $\chi_{ijk\ldots}^{(2n)}$, which is responsible for nonlinear processes such as second harmonic generation and three wave mixing, must be zero: this is immediately seen by reversing the direction of the electric field in Eq.(1) (that is $\underline{E} \to -\underline{E}$) and observing that, because of the symmetry of the medium, the polarization produced by it must bear the same relationship to the field, that is $\underline{P}$ must become $-\underline{P}$, so that the lowest significant nonlinear term is the cubic one $\underline{P}^{(3)}$. This term is responsible for a number of nonlinear effects, the most important of which turn out to be, as far as optical fibers are concerned, stimulated Raman scattering, stimulated Brillouin scattering and optical Kerr effect (intensity-dependent refractive index). Other processes which are in principle possible, as third harmonic generation and parametric four-photon interaction, require phase matching and their efficiency is usually (unless special phase-matching techniques are utilized) much smaller than that of the previous ones.



The analytical description of a given nonlinear process is usually accomplished by assuming the spectrum of the field to consist of a discrete set of frequencies and by working out the nonlinear polarization as the result of the mixing of three monochromatic waves. Thus, for example, the description of a given Raman (or Brillouin) line with frequency $\omega_r$ (see Fig.2) requires that we keep only those terms of $\underline{P}^{(3)}$ which contain products of the form

$$E_p E_p E_r \qquad (5)$$

where $E_p$ refers to the electric field of the pump wave and $E_r$ to that of the electric field of the wave at the Raman frequency, and, of these terms, only those that exhibit a harmonic dependence of the kind $\exp(\pm i\omega_r t)$. These contributions are then inserted as source term in the nonlinear wave-equation which describes the evolution of the wave at the frequency $\omega_r$.

## Raman and Brillouin scattering

Raman scattering consists in the appearance of weak sidebands in the spectrum of an electromagnetic beam traveling in a dielectric medium (see Fig.3), the spacing of the sidebands being determined by the vibrational resonant frequencies of the dielectric material. Brillouin scattering is a special case of Raman scattering involving interaction with thermally excited acoustic waves. A fully quantized description of the process shows that there are both spontaneous and stimulated emissions of photons at the sideband frequencies, giving rise to stimulated Raman and Brillouin scattering (SRS and SBS). They can be classically viewed as coupled three-wave interaction

involving an incident pump wave, a generated vibrational or acoustical wave and a scattered signal wave at the Stokes frequencies (light at anti-Stokes frequencies usually suffers loss). As a consequence, the energy initially contained in the pump is progressively transferred to the signal wave, in both the forward and backward directions for SRS and, because of wavevector matching considerations, only in the backward direction for SBS. We have already appreciated the effect of the presence of the waveguide on the efficiency of the nonlinear processes, which essentially amounts to ignore diffraction effects and to substitute the cross area of the beam with the area of the core and are accordingly able to understand the relevance of the above mechanism in optical communication systems: in fact, also if no Stokes signal field is deliberately injected into the fiber, the weak signal due to spontaneous emission can be significantly amplified and thus subtract power from the information carrying pump-wave.

Stimulated Raman and Brillouin scattering are usually characterized by small-signal gain coefficients $G_R(\nu)$ and $G_B(\nu)$ which represent, neglecting pump depletion, the exponential gain of the spectral intensities $I_R(z,\nu)$ and $I_B(z,\nu)$ of the signal at frequency $\nu$, that is

$$I_R(z,\nu) = I_R(0,\nu) \exp\left[G_R(\nu) z\right] , \qquad (6)$$

$$I_B(z,\nu) = I_B(0,\nu) \exp\left[G_B(\nu) z\right] . \qquad (7)$$

Since both gain coefficients are proportional to the pump intensity $I_0$, it is customary to introduce the quantities

$$g(\Delta\nu) = G(\nu)/I_0 \qquad (8)$$

where $\Delta\nu = \nu_0 - \nu_S$ is the difference between the pump frequency $\nu_0$ and the



Stokes-line frequency $\nu_S$.

The gain coefficient $g_R(\nu)$ is plotted in Fig.4 for fused silica: note that, because of the complexity of the molecular structure of glass, the vibrational levels form a continuous band and so do the Stokes lines. Brillouin frequency shifts $\nu_B$ are small (of the order of 1 $cm^{-1}$, $\nu_B = 2Vs\ \nu_p/c$ with Vs the sound velocity) as compared to Raman shifts ($\sim 400\ cm^{-1}$) and, besides, Brillouin linewidths are sharp ($\sim 100$ MHz) and vary approximately with the square of the pump frequency $\nu_p$ ($\Delta\nu_B = 38.4/\lambda_p^2$ MHz). Raman bands are broad ($\sim 300\ cm^{-1}$) and their width and frequency shift does not vary with pump frequency. The peak Brillouin gain is more than two order of magnitude larger than the peak Raman gain but, if the pump linewidth $\Delta\nu_p$ is larger than $\Delta\nu_B$, its effective value is reduced by the ratio $\Delta\nu_B/\Delta\nu_p$.

Future long-distance wideband communication systems are going to employ narrow linewidth laser ($\lesssim 100$ MHz) and, in particular, coherent transmission systems will require extremely narrow laser-bandwidth ($\lesssim 1$ MHz). These conditions precisely favour SBS and if the power launched into the fiber exceeds some critical power level (this critical power $P_c$ can be defined, both for SBS and SRS, as that for which the Stokes power increase from noise to equal the pump power), a significant portion of it may be converted into a Brillouin signal-wave traveling backward (see Fig.5) which is detrimental to the telecommunication system in many ways (the introduction of an increase in signal attenuation being the most obvious).

By assuming for $P_c$ the expression

$$P_c^{(B)} \simeq 4.4 \times 10^{-3}\, d^2 \lambda^2 \xi\, \Delta\nu_B \quad \text{watts} \qquad (9)$$

where the wavelength $\lambda$ and the core diameter are in $\mu m$, $\xi$ is the fiber loss

in dB/km and $\Delta\nu_B$ is in GHz, one obtains for a typical monomode fiber for long-distance loss-limited telecommunications (d=5 $\mu$m, $\lambda$=1.5 $\mu$m, $\xi$=0.33 dB/Km) and a nearly monochromatic transmitter (linewidth 130 MHz) a critical power of the order of 10 mW. The limitation which this figure sets on the transmissible power can be eliminated by broadening the transmitted spectrum (as we have already pointed out the gain coefficient is in this case reduced by the ratio $\Delta\nu_B/\Delta\nu_p$) so that its spectral density is less than about 0.1 mW/MHz, a condition which can be satisfied with a noisy laser having sufficient incidental frequency modulation. Possible alternative techniques for suppressing SBS during transmission of narrow-band laser light are based on the principle of intentionally imposing a suitable phase modulation on the optical field produced by a laser transmitter with linewidth $\Delta\nu_L << \Delta\nu_B$, so as to reduce the SBS gain. SRS presents a much more difficult problems, also in view of the fact that its critical power is relatively independent of the transmitter spectral width,

$$P_c^{(R)} \simeq 5.9 \times 10^{-2} d^2 \lambda \xi \quad \text{watts}. \qquad (10)$$

Also if this power threshold is significantly larger than that of SBS (with the same figures given above one gets $P_c^{(R)} \simeq 0.73$W) and Raman amplification takes place in both forward and backward directions, it constitutes, because of the progressive conversion of the injected power from the transmission wavelength to the longer Stokes-shifted wavelengths, a serious limitation to WDM (wavelength division multiplexing) techniques. It has been estimated that if the telecommunication channels are spread uniformly over a bandwidths of 40-100 nm, then a total launched power exceeding 40 mW can add a loss larger than 1 dB.



Fiber Raman and Brillouin lasers

If the power fed into the fiber is large (or the fiber sufficiently long) there will always be some spontaneous Raman scattering which will allow to see, because of stimulated scattering, a significant output of Stokes lines which can be amplified to intensities comparable to that of the pump. With reference to Fig.6, which represents a schematic set-up of a typical Raman scattering experiment, the output consists of several Stokes orders, dispersed by a prism: in fact, if the Stokes power within the fiber is high enough, it can act as a pump for the next Stokes order and sequential conversion to successive orders can take place (see Fig.6 bis). Even in this simple single pass configuration, a Raman amplifier is able to generate a series of pulses in the region 1.1-1.5 $\mu$m pertinent to fiber characterization.

By the introduction of a feedback, both Raman and Brillouin oscillators (either CW or pulsed) can be realized as shown in Fig.7. In particular, a CW Raman laser can be tuned over a range of approximately 240 $cm^{-1}$ (see Fig.4). Threshold powers for CW Raman lasers are in the range 50-200 mW, depending on the pump wavelength.

SBS lasers possess, thanks to the narrow line width excitation, a lower threshold which can be in the submilliwatt range in the ring configuration.

Optical Kerr effect

The nonlinear response of the fiber material (silica or fused quartz) at optical frequencies is dominated by fast responding electronic processes. If the resonant frequencies of the electronic transitions are assumed to be well

above any of the interacting frequencies, then the polarization responds instantaneously to the field and, by assuming the material to be isotropic, the third order polarizability can be written as

$$\underline{P}^{(3)} = \varepsilon_0 \chi^{(3)} \underline{E} \cdot \underline{E} \; \underline{E} \qquad (11)$$

where $\varepsilon_0$ is the electric permeability of vacuum and $\chi^{(3)}$ the nonlinear susceptibility.

The optical Kerr effect is associated with those contributions in Eq.11 which vibrate at (approximately) the same frequency of the field (or exactly at its frequency in the monochromatic field case). If the field is linearly polarized, these can be shown to be equivalent to the introduction of a nonlinear contribution to the refractive index according to the relation

$$n(\omega) = n_1(\omega) + n_2 |\hat{\underline{E}}|^2 \qquad (12)$$

where $\hat{\underline{E}}$ is the analytic signal of the field (and, thus, $|\hat{\underline{E}}|$ its peak value) and $n_2$, the nonlinear refractive index coefficient, is with good approximation independent from $\omega$. Eq.(12) can also be rewritten in term of the intensity I as

$$n(\omega) = n_1(\omega) + N_2 I \qquad (13)$$

where $N_2 = 2(n_2/n_1)(\mu_0/\varepsilon_0)^{1/2}$, typical values for silica being $N_2 = 5 \times 10^{-16}\ cm^2/W$ (corresponding to $n_2 = 10^{-22}\ m^2/V^2$).

The nonlinear contribution to the refractive index appearing in Eq.(12) affects both the transverse and the longitudinal behavior of propagating beam. The fact that, if $n_2 > 0$ as in silica, the refractive index at the center of the beam is larger than at the periphery, gives rise to a self-guiding mechanism which is known as self-focusing. This effect is usually negligible in glass fibers where, conversely, the longitudinal effects are relevant.



## Self-phase modulation, pulse compression and soliton propagation

The longitudinal effects described in this section are associated with the competition existing between the linear and nonlinear parts of the refractive index n in determining the evolution of a light pulse. The linear part $n_1(\omega)$ is responsible for the dispersive properties of the medium, that is for the fact that different frequencies travel at different velocities. More precisely, if one considers the components of the em field propagating along the z-direction around a given frequency $\omega$ in a small interval $\delta\omega$

$$\int_{\omega-\delta\omega}^{\omega+\delta\omega} E_{\omega'} e^{-iK(\omega')z + i\omega' t} \, d\omega' \quad , \quad K(\omega) = \frac{\omega}{c} n(\omega) \quad , \qquad (14)$$

they travel at a common group-velocity

$$V(\omega) = \left(\frac{dK}{d\omega}\right)^{-1} \qquad (15)$$

so that, if the field possesses a spectrum of finite width $\Delta\omega$,

$$\int_{\omega_0-\Delta\omega}^{\omega_0+\Delta\omega} E_\omega e^{-iK(\omega)z + i\omega t} \, d\omega \quad , \qquad (16)$$

this mechanism gives rise to a delay among the slow and fast frequencies (and thus to a pulse broadening) characterized by the so-called group-velocity dispersion (GVD)

$$A = \left.\frac{d^2K}{d\omega^2}\right)^{-1}_{\omega=\omega_0} . \qquad (17)$$

The nonlinear part is responsible for a self-phase modulation since its influence can be described (as a first approximation) by considering $N_2 I$ (see Eq.13) as an actual refractive index and thus replacing the linear propagation constant $K(\omega)$ with the expression

$$K(\omega) + \frac{\omega}{c} N_2 I \qquad (18)$$

which implies the frequency components of the field to evolve as

$$E_\omega \, e^{i\kappa(\omega) z + i \frac{\omega}{c} N_2 I z - i\omega t} \quad . \tag{19}$$

It is then apparent that, in the regime of negative group-velocity dispersion (or anomalous GVD, $\lambda \gtrsim 1.3 \mu m$ for silica) where

$$A < 0 \quad , \tag{20}$$

an optical pulse tends to be compressed by its nonlinear interaction with the medium. As a matter of fact, since the group velocity is in this case an increasing function of $\omega$ ,

$$\frac{d}{d\omega} V(\omega) = - V^2/A \quad , \tag{21}$$

the leading edge of the pulse, which according to Eq.20 is down-shifted in frequency, tends to travel at a lower velocity than the trailing edge which is conversely up-shifted in frequency (see Fig.8). Obviously the same argument if applied to the case of positive group velocity dispersion ($A > 0$, normal GVD) would imply a broadening of the pulse.

The theory of pulse propagation in a single-mode optical fiber in the presence of the optical Kerr effect describes the above process by means of a nonlinear differential equation (sometimes improperly called nonlinear Schrödinger equation). Considering, for simplicity, a single-mode polarization maintaining fiber whose field reads

$$\underline{E}(\underline{r}, z, t) = \mathcal{E}(\underline{r}) \, e^{i\omega_0 t - i\beta(\omega_0) z} \, \phi(z,t) \, \hat{x} \quad , \quad \underline{r} \equiv (x, y) \, , \tag{22}$$

where $\omega_0$ represents the (average) frequency of the carrier, this equation is

$$\left( \frac{\partial}{\partial z} + \frac{1}{V} \frac{\partial}{\partial t} \right) \phi - \frac{i}{2A} \frac{\partial^2}{\partial t^2} \phi = - i R |\phi|^2 \phi \tag{23}$$

where

$$R = (\omega_0 n_2 / c) \iint_{-\infty}^{+\infty} \mathcal{E}^4(\underline{r}) \, dx \, dy \equiv (\omega_0 n_2 / c \sigma) \, , \tag{24}$$

$$V = \left( d\beta / d\omega \right)^{-1}_{\omega = \omega_0} \, , \quad A = \left( d^2\beta / d\omega^2 \right)^{-1}_{\omega = \omega_0} \, . \tag{25}$$



In Eq.(24) $\mathcal{E}(\underline{r})$ is normalized to one, that is

$$\iint_{-\infty}^{+\infty} \mathcal{E}^2(\underline{r}) \, dx \, dy = 1 \quad , \tag{26}$$

so that $\sigma$ has the physical dimension of an area (effective area of the mode); with good approximation

$$\sigma = \pi a^2 / \ell n \, v$$

where $a$ is the core radius and $v$ the fiber normalized frequency.

It is easy to prove that Eq.(23) admits of the two exact analytical solutions

$$\phi(z,t) = e^{i\chi z} \, \phi_0 \, \mathrm{sech} \left[ (t - z/V)/\tau_0 \right] \quad , \quad \left( \mathrm{sech} \equiv \frac{1}{\cosh} \right) \, , \tag{27}$$

(bright envelope-soliton)

and

$$\phi(z,t) = e^{i\chi z} \, \phi_0 \tanh \left[ (t - z/V)/\tau_0 \right] \, , \tag{28}$$

(dark envelope-soliton) ,

where $\tau_0$ is an arbitrary scale which is taken to be the temporal pulse width, provided that the following relations are respectively verified:

$$\begin{cases} 2A\tau_0^2 \chi = 1 \\ A \tau_0^2 R |\phi_0|^2 = -1 \end{cases} \tag{29}$$

and

$$\begin{cases} A\tau_0^2 \chi = -1 \\ A \tau_0^2 R |\phi_0|^2 = 1 \end{cases} \quad . \tag{30}$$

Bright solitons corresponds to the effective propagation of a light pulse, dark solitons to the propagation of the absence of signal (see Fig.9). Note that bright soliton propagation can be achieved only in the anomalous dispersion regime, while dark soliton propagation requires $A>0$. Referring below to the (more interesting) case of $A<0$, and after introducing the dimensionless

variables

$$\begin{cases} \xi = z/|A|\tau_0^2 \\ s = (t - z/v)/\tau_0 \\ u = \tau_0 (R|A|)^{1/2}\Phi \end{cases} \qquad (31)$$

Eq.23 can be rewritten in the dimensionless form

$$\frac{\partial u}{\partial \xi} - \left(\frac{i}{2}\right)\frac{\partial^2 u}{\partial s^2} = -i|u|^2 u \ . \qquad (32)$$

It is possible to prove that, besides the fundamental soliton described by Eq.(27), there are a number of higher-order solitons which develope structure periodically in z corresponding to input pulses of hyperbolic secant shape and amplitudes integral multiples of the amplitude of the fundamental soliton. Referring to the adimensional variables, all solitons are excited by the input pulses of the kind

$$u(\xi = 0, s) = M\,\mathrm{sech}(s) \qquad (33)$$

the integer M being the order of soliton (the fundamental soliton corresponding to M=1). It is possible to give analytic expressions only to the two first solitons and they read

$$u_1(\xi, s) = e^{-i\xi/2}\,\mathrm{sech}(s) \ , \ (\text{see Eq. 27}) \ , \qquad (34)$$

and

$$u_2(\xi, s) = \frac{4e^{-i\xi/2}[\cosh(3s) + 3e^{-4i\xi}\cosh(s)]}{\cosh(4s) + 4\cosh(2s) + 3\cos(4\xi)} \ . \qquad (35)$$

All the solitons (with the exception of the fundamental one) have a common period $\xi_0 = \pi/2$ or, in the z variable,

$$z_0 = (\pi/2)|A|\tau_0^2 \ . \qquad (36)$$

In Fig.10 is shown a perspective plot of the temporal pulse shape at various points along the fiber for the M=3 soliton. From this behavior, one can induce that an optimal pulse narrowing will occur at certain fiber lengths. The power necessary to generate a soliton is given, in MKS units, by the expression

$$P = \left(\frac{n_1}{g}\right)\left(\frac{\varepsilon_0}{\mu_0}\right)^{1/2}\frac{\lambda M^2 \sigma}{z_0 n_2} = \left(\frac{\lambda}{4}\right)\frac{M^2\sigma}{z_0 N_2} \ . \qquad (37)$$

The soliton period $z_0$ can be expressed in terms of the chromatic delay $T_{cr}$ of the fiber through the relation

$$z_0 = \pi^2 c\,\tau_0^2/T_{cr}\lambda^2 \ . \qquad (38)$$

Typical values of $T_{cr}$ are 5÷15 psec/Km nm while $\tau_0$ can be made of the order of 3÷4 psec; for $\lambda \simeq 1.5\,\mu m$, this furnishes $z_0 \simeq 1.3$ Km. The power $P_1$ necessary to generate the fundamental soliton is of the order of 1 W; also, for typical core size (a=3-4$\mu$m) of monomode fibers, the following relation holds true between $P_1$ and the period $z_0$ (in kilometers):

$$P_1 \simeq \frac{1}{z_0} \ \text{watts} \ . \qquad (39)$$

## Pulse compression in the regime of normal GVD

The previous considerations makes clear that at wavelengths of anomalous GVD the fiber acts as a pulse compressor (soliton compression). Fig.11 displays pulse shapes for several values of initial pulse amplitude at the point of optimal narrowing. Note that also if the pulse can be greatly narrowed (to picoseconds), there is usually a broad pedestal that contains about as much energy as the narrow spike itself so that the pulse quality (defined as $I_{peak}\tau/\tau_0$, where $I_{peak}$ is the peak intensity of the compressed pulse relative to that of the input pulse and $\tau$ the FWHM of the compressed pulse) is rather poor (~0.2). A more versatile approach consists in letting a short optical pulse to propagate through a single-mode fiber in the regime of positive GVD. During the passage through the fiber, both the pulse shape and frequency

bandwidth are broadened and, under easily achieved conditions of pulse intensity and fiber length, the entire pulse can be positively linearly chirped: this enhanced frequency chirp enables the output pulse to be subsequently compressed by a pulse compressor (typically a grating pairs which can be schematized as a delay line with a frequency dependent delay) to very short width (as short as tens of femtoseconds).

In Fig.12, a perspective plot of the pulse temporal shape is shown for various fiber lengths in the case of positive GVD. The steep-lope leading and trailing edge of the pulse generate, through the optical Kerr effect, additional frequencies, the resulting broadening of the spectral width being shown in Fig.13. Because the new frequencies are mainly created at the leading and trailing edges, which gradually move apart in time, the pulse develops a frequency chirp linear in time, which is plotted in Fig.14. A pulse with such a characteristic has a temporal phase proportional to $t^2$ so that its Fourier transform has a phase proportional to $\omega^2$. A quadratic compressor (as a grating-pair compressor) which has a delay function of the form

$$\Psi(\omega) = \Psi_0 - \alpha \omega^2 \qquad (40)$$

with the constant $\alpha$ easily adjusted by varying the grating separation, is thus the ideal compressor since it will be able to cancel the phases of the frequency components of the pulse and leave them in phase so to create a pulse with the maximum possible peak amplitude. In Figs.15 and 16 are respectivelyt plotted the compression factor (defined as the ratio of the FWHM of the input pulse to that at the output pulse) and the pulse quality as a function of the fiber length for various values of the input intensities.

The output pulse from a grating compressor can be fed into an other fiber



and compressor, thus realizing a two-stage compressor. The compression achievable in the second stage is however substantially less than that achievable in the first and compressors with more than two stages are not likely to be used.

Solitons in optical communications

The possibility of a dispersionless transmission based on soliton propagation comes naturally to the mind and induces to speculate about the possibility of achieving broad band information transmission rate over long distances. One does not need to think only in terms of the fundamental soliton $M = 1$ since by lenghtening the input pulse $\tau_0$ and by reducing the chromatic delay $T_{cr}$, the soliton period can be easily stretched (see Eq.(38)) to many tens of kilometers, with a corresponding reduction of the intensities required for solitons (see Eq.(39)). A further reduction of the peak power can be obtained, by reducing the core diameter, to the order of tens of mW and so within the capacity of existing semiconductor lasers.

There are of course remaining fundamental questions associated with the fact that the propagation distances are significantly larger than the decay length of the energy in the pulse (for a 0.2 dB/Km loss, the total loss in 30 Km will be 6 dB, that is a four times reduction in power) and that, in any realistic system, it may not be possible to launch into the fiber an initial pulse of the form necessary to generate a soliton (see Eq.(33)).

Both experimental and numerical results seems to indicate that one is always able to observe pulse narrowing, in spite of the large loss as if the pulse would retain the feature of the initial pulse even after its intensity

decreases. As far as the second question is concerned, the theory tells that in general the behavior of the solution $u(\xi, s)$ of Eq.(32) consists of a soliton and of a continuum of modes which die off asymptotically for large $\xi$ : the order of this soliton is determined by the value of the area

$$A = \int_{-\infty}^{+\infty} |u(0,s)|^2 ds \qquad (41)$$

and it is obtained by the closest integer N which satisfies the relation

$$A + \frac{1}{2} \geq N \ . \qquad (42)$$

By utilizing the above results, transmission systems with optimum transmission rate and minimum required power can be designed with an achievable bit rate an order of magnitude better than the best linear transmission.

Essential references

Raman and Brillouin scattering:


1. R.H.Stolen: "Nonlinearity in fiber transmission", Proc.IEEE 68, 1232(1980)
2. R.H.Stolen: "Active fibers", New Directions in Guided Wave and Coherent Optics", Vol.I, ed. by D.B.Ostrowsky and E.Spitz, M.Nijhoff Publ., The Hague, 1984

Optical Kerr effect

3. A.OwYoung, "The origins of nonlinear refractive indices of liquids and glasses", Ph.D. Thesis (California Institute of Technology, Pasadena, Cal. 1971), unpublished
4. B.Crosignani, "Self-induced nonlinear effects in optical fibers", in "New Directions in Guided Wave and Coherent Optics", Vol.I, ed. by D.B.Ostrowsky and E.Spitz, M.Nijhoff Publ., The Hague, 1984
5. W.J.Tomlinson, R.H.Stolen and C.V.Shank, "Compression of optical pulses chirped by self-phase modulation in fibers", J.Opt.Soc.Am. B1 , 139 (1984)
6. A.Hasegawa and Y.Kodama, "Signal transmission by optical solitons in monomode fiber", Proc. IEEE 69, 1145 (1981)

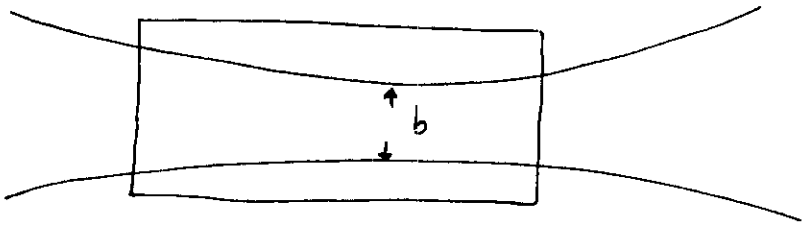


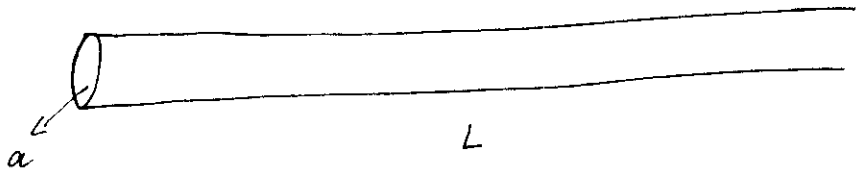


Fig. 1 : Geometry of the nonlinear interaction in a bulk medium and in a dielectric waveguide.



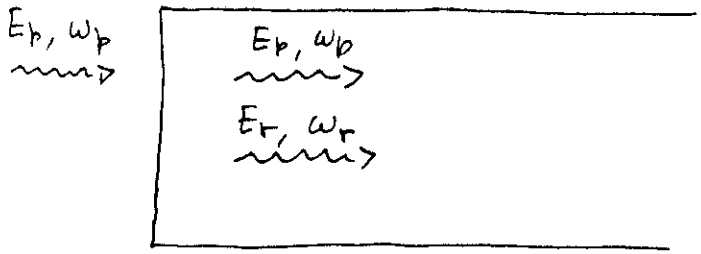


Fig. 2 : Schematic of Raman scattering in which a single line at frequency $\omega_r$ is generated.


Fig. 3 : Stokes and anti-Stokes frequencies generated by the pump at frequency $\omega_p$.

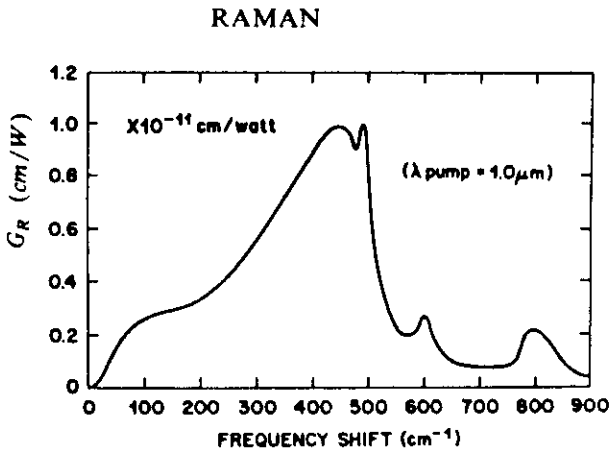


Fig. 4 : Raman gain curve.

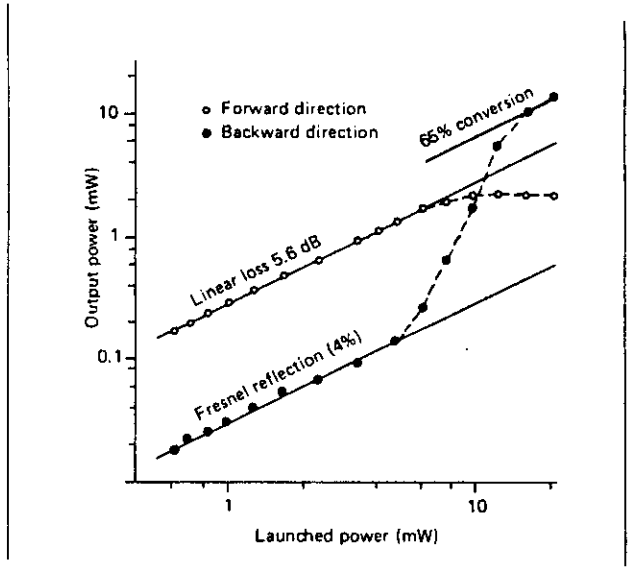


Fig. 5 : Power emitted from the forward and backward ends of a 13.6 Km monomode fiber as a function of launched power at 1.32 μm.

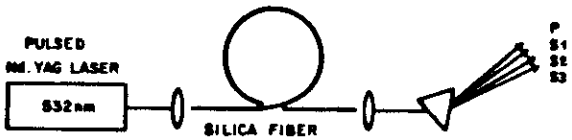


Fig. 6 : Schematic arrangement for observing the development of the stimulated Raman spectrum.



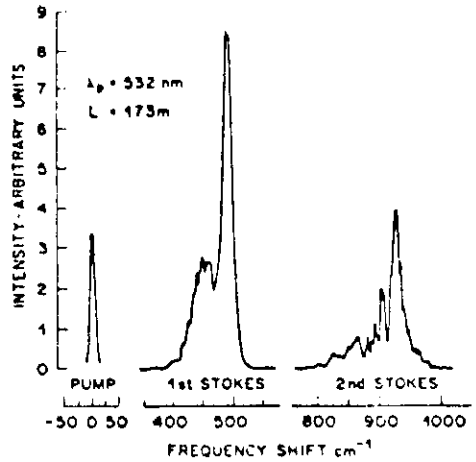


Fig. 6a : First and second Stokes spectra pumped by a Q-switched Nd:YAG laser.

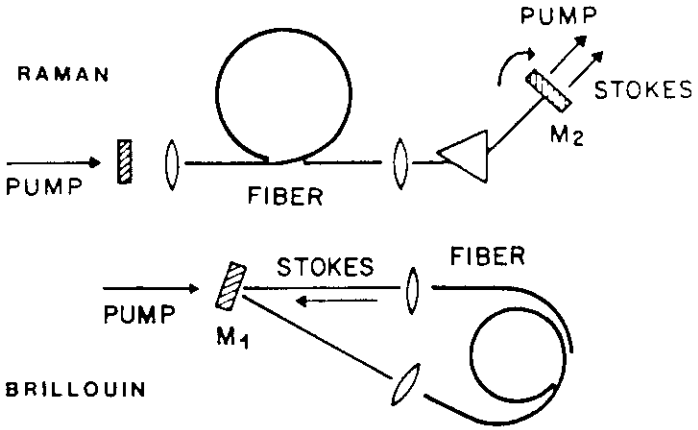


Fig. 7 : Tunable fiber Raman laser and Brillouin ring laser.



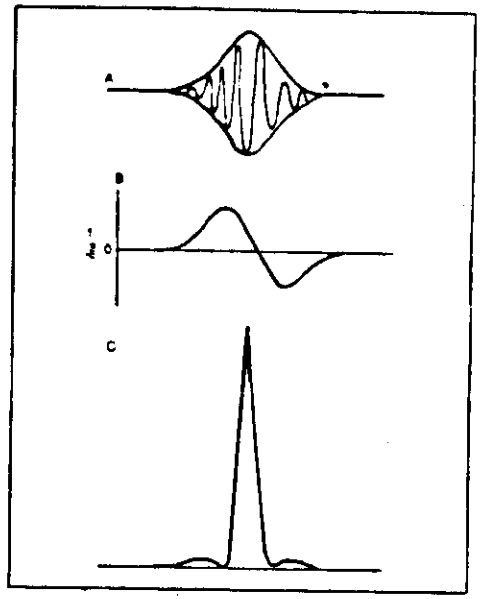


Fig. 8 : Optical pulse experiencing self-phase modulation with corresponding frequency chirp ald pulse compression.

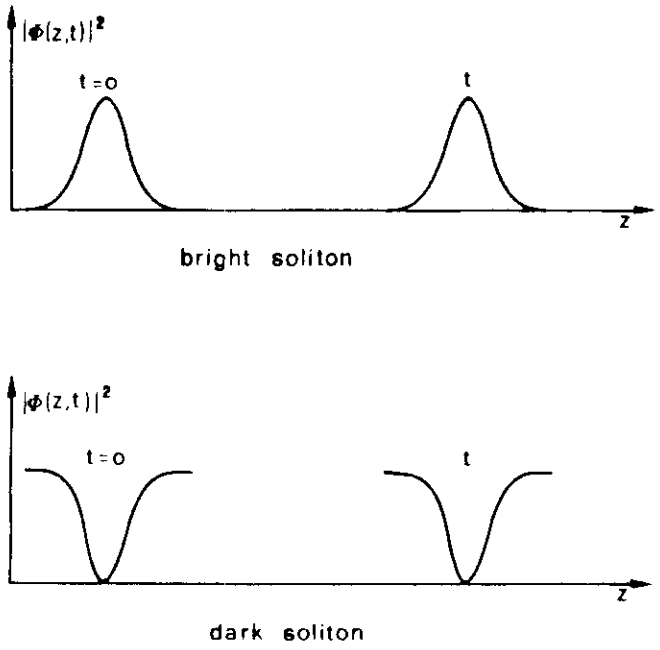


Fig. 9 : Fundamental bright and dark soliton propagation.



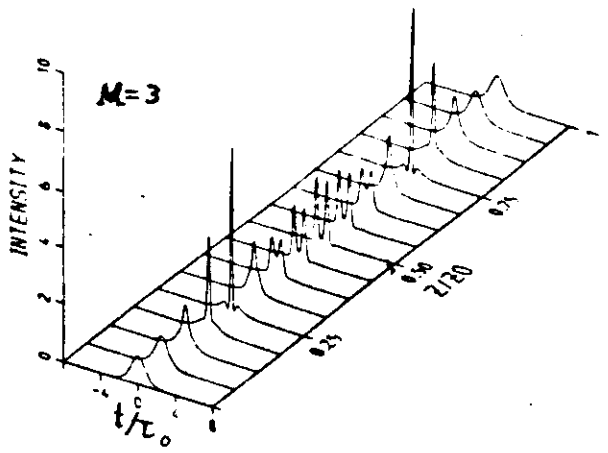


Fig. 10 : Perspective plot of temporal pulse shape at various points along the fiber for the M=3 soliton.

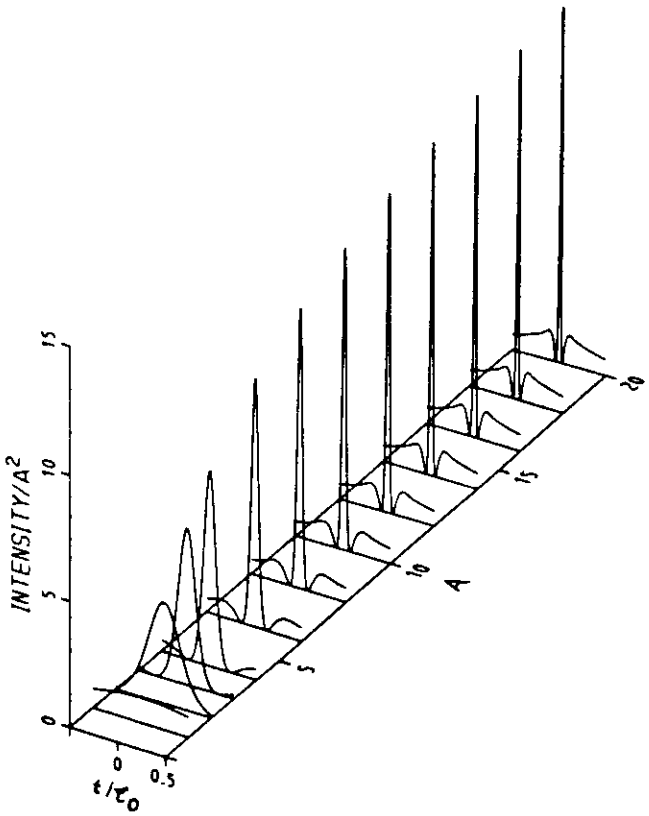


Fig. 11 : Calculated pulse shapes for soliton compression at the point of optimal narrowing.



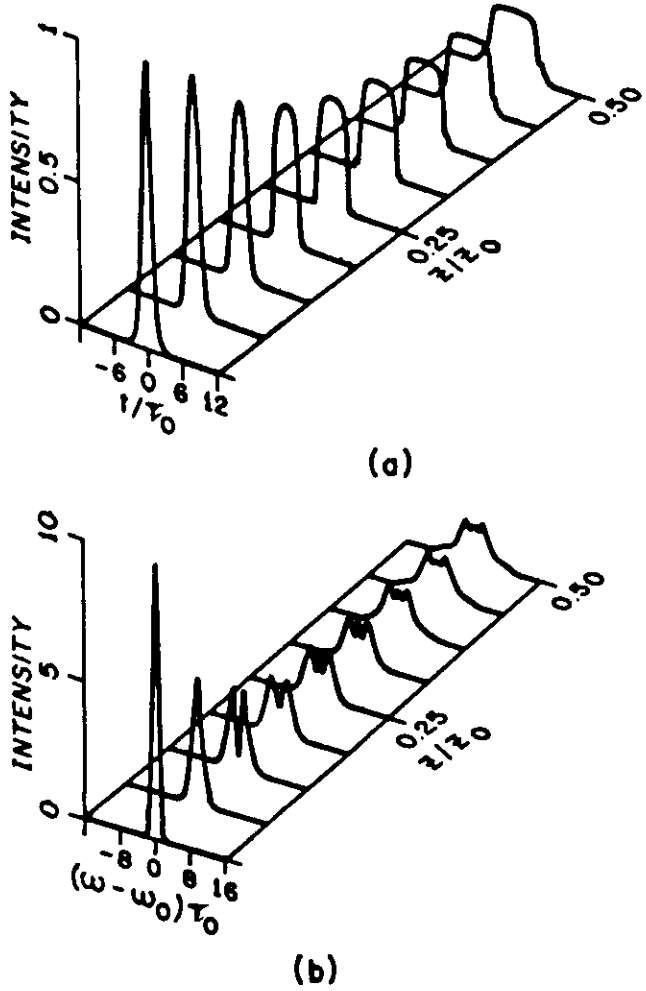


Fig. 12 (top) : Perspective plot of the temporal shape of a pulse for positive GVD.

Fig. 13 (bot.): Perspective plot of the spectral shape of a pulse for positive GVD.

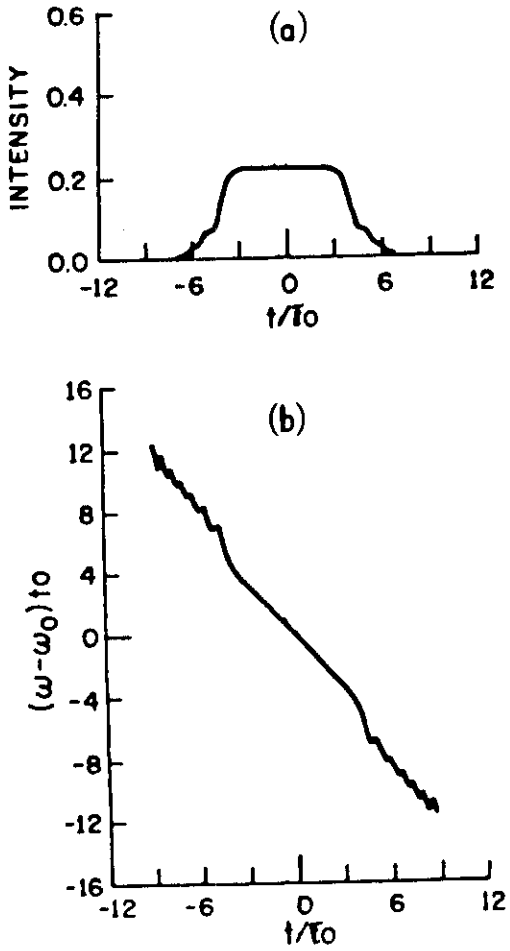


Fig. 14 : Pulse intensity as a function of time for $z/z_o = 0.5$ (a); instantaneous frequency as a function of time (b).

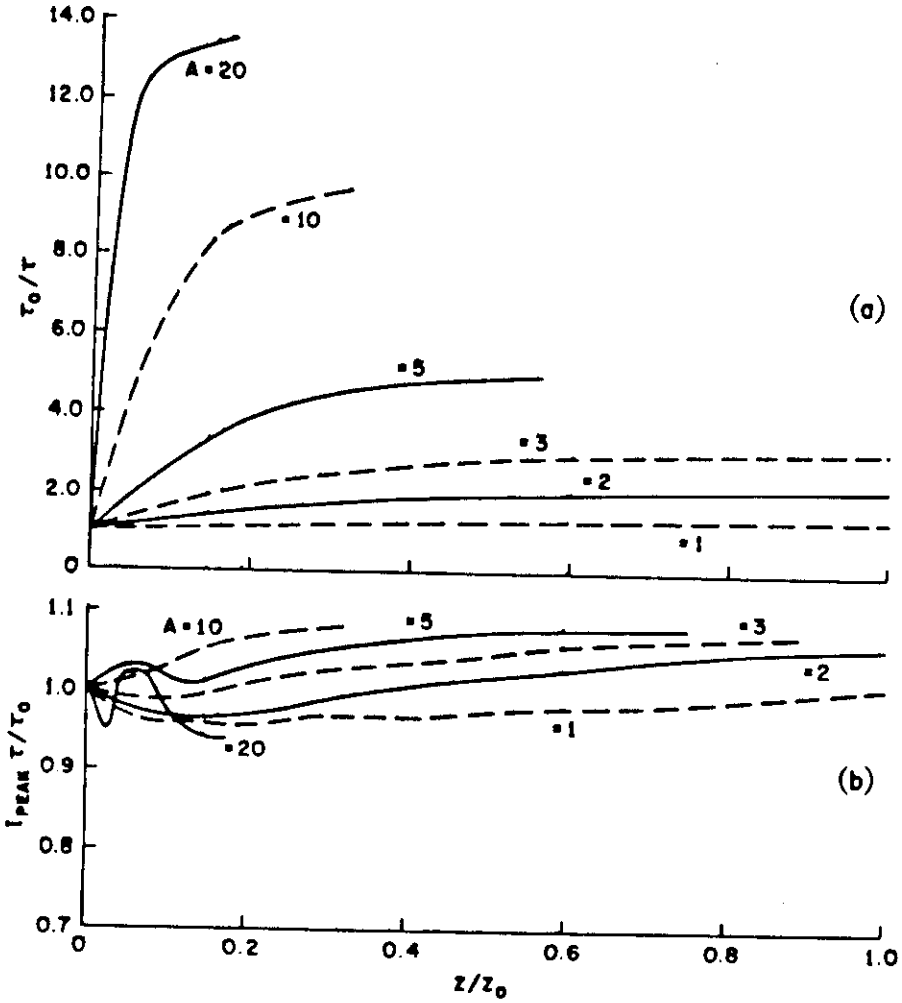


Fig. 15 (top) : Pulse compression as a function of fiber length for various normalized pulse amplitudes.

Fig. 16 (bot.): Quality factor.